

Isotopic differentiation and sublattice melting in dense dynamic iceAndreas Hermann,^{1,2,*} N. W. Ashcroft,³ and Roald Hoffmann²¹*School of Physics and Astronomy and Centre for Science at Extreme Conditions, The University of Edinburgh, Edinburgh, EH9 3JZ, United Kingdom*²*Department of Chemistry and Chemical Biology, Cornell University, Ithaca, New York 14853, USA*³*Laboratory of Atomic and Solid State Physics, Cornell University, Ithaca, New York 14853, USA*

(Received 20 June 2013; published 27 December 2013)

The isotopes of hydrogen provide a unique exploratory laboratory for examining the role of zero point energy (ZPE) in determining the structural and dynamic features of the crystalline ices of water. There are two critical regions of high pressure: (i) near 1 TPa and (ii) near the predicted onset of metallization at around 5 TPa. At the lower pressure of the two, we see the expected small isotopic effects on phase transitions. Near metallization, however, the effects are much greater, leading to a situation where tritiated ice could skip almost entirely a phase available to the other isotopomers. For the higher pressure ices, we investigate in some detail the enthalpies of a dynamic proton sublattice, with the corresponding structures being quite ionic. The resistance toward diffusion of single protons in the ground state structures of high-pressure H₂O is found to be large, in fact to the point that the ZPE reservoir cannot overcome these. However, the barriers toward a three-dimensional coherent or concerted motion of protons can be much lower, and the ensuing consequences are explored.

DOI: [10.1103/PhysRevB.88.214113](https://doi.org/10.1103/PhysRevB.88.214113)

PACS number(s): 62.50.-p, 71.15.Pd, 71.15.Mb, 63.20.dk

The first and third most abundant elements in the universe combine to form H₂O: water in its fluid form and ice in the crystalline or amorphous forms. The phases of the crystalline ices are remarkably rich in their structures.¹ Recent studies on stable high pressure phases of ice have uncovered a variety of new phases that become stable at pressures beyond $P = 1$ TPa (1000 GPa, or 10 Mbar).^{2–6} There is now an understanding that the electronic band gap of ice is not likely to close until pressures reach around $P = 5$ TPa (corresponding to a compression of roughly $V_0/V = 11.5$), where metallic ice phases actually first become more stable than all known insulating phases. The stable ice phases at these pressures are notably more complex than, e.g., the highly symmetric phase ice *X*, which becomes stable around $P = 100$ GPa and which features symmetric and linear O-H-O bridging bonds.¹

Hydrogen (atomic mass 1) and oxygen (mass 16) are both comparatively light elements, and the zero point energies (ZPEs) at megabar pressures are exceedingly large, on the order of 1–1.5 eV per H₂O unit in the harmonic approximation.⁶ The question thus arises as to whether the associated motions in the ground state of ice under these conditions could lead to a diffusional, a superionic, or even a fully fluid phase. These states of matter of ice are of great astrophysical interest because of the presence of H₂O, one of the thermodynamic sinks of all worlds,⁷ in the interior of giant gas planets.^{8–12} However, the corresponding environments usually combine high pressures with very high temperatures, and this hot, or near-classical, melting of ice is quite different from the cold, or even quantum, melting associated purely with zero point vibrational excursions and which is of especial interest here.

Water ice is special because of its relatively high hydrogen content—and hydrogen, with the isotopes H, D, and T, can vary its mass by a factor of three, a range unknown for any other element (although in what follows it is notable that the oxygen isotopes themselves already cover a range of atomic mass from 12 to 24 [Ref. 13]). In terms of fundamental quantum statistics, protium is a Fermion, deuterium is a Boson, and tritium once again is a Fermion. Heavy water, D₂O, was utilized as a

neutron moderator in early nuclear power reactors and is today widely used in organic chemistry as a deuterium source for nonradioactive isotopic labeling of substances and in neutrino detectors because of the enhanced interaction cross-section of neutrinos with deuterium. The heaviest hydrogen isotope, tritium, is radioactive with a half-life of about 12.3 years. It finds its utility as a radioactive isotopic label or in studies of isotopic effects.¹⁴ Tritium is produced by various reactions in nuclear reactors but also, for instance, by highly energetic cosmic neutron rays interacting with nitrogen in the upper atmosphere.^{15,16}

It may be pertinent to ask whether the extreme conditions of pressure we study (while certainly present in nature, e.g., in the interior of giant planets¹⁷ and possibly involved in exotic phenomena such as icy volcanoes¹⁸) are accessible to experiments. It should then be pointed out that current experimental capabilities in static compression using diamond anvil cells have reached the 0.3 TPa range (for some systems, as high as 0.6 TPa¹⁹), that neutron diffraction on ice samples is possible up to about 0.1 TPa (100 GPa),²⁰ and that shock wave compression experiments have reached the multi-TPa pressure regime (albeit along the Hugoniot, which is at very high temperatures).²¹ Ramp compression experiments (with possible precompression in diamond anvil cells) promise to reach similar pressures but at much lower temperatures.²²

While D₂O is more or less readily available to researchers, tritium oxide (T₂O) is less likely to be a subject of experimental study;²³ however, in a theoretical and computational *Gedankenexperiment*, we can use T₂O and D₂O along with the common isotopomer H₂O to create, as noted above, a small laboratory in which ZPEs are tuned in a discrete manner to probe the dynamics of ice structures. Can the significant zero point effects in ice under high pressure cause quantum melting of the hydrogen sublattice? How would this be affected by the mass of the hydrogen isotope? Can isotopic substitution change phase stability boundaries? Can it influence the existence of a possible superionic or quantum liquid state of ice?

We start by using the structures presented in our recent work⁶ to study the changes in the phase boundaries that might occur if all H atoms were to be replaced by D or T atoms. To do this, we need to estimate the zero point vibrational energies and corresponding average displacements associated with each structure over the pressure range of interest. Here, we restrict ourselves to the harmonic approximation to the vibrational problem (the applicability of which we will discuss below), hence decoupling the nuclear from the electronic motion and, more importantly, treating all nuclei as point particles moving on a potential energy surface, as given by the electronic ground state. In principle, for example, an extension toward the self-consistent harmonic approximation is feasible.^{24–27} We use the PHON and PHONOPY programs together with the Vienna *Ab initio* Simulation Package to calculate interatomic force constants to set up the dynamical matrix and then diagonalize it on a fine grid of the Brillouin zone to obtain the phonon frequencies and their corresponding densities of states.^{28–30} The computational details are similar to those utilized in our previous study.⁶ At the harmonic level, isotopic effects influence only the eigenvalues and vectors of the dynamical matrix but do not influence the force constants. This is in some contrast to, e.g., the self-consistent phonon approximation mentioned above.

I. ISOTOPE AND PRESSURE EFFECTS ON ZPES

To illustrate the influence the different isotopes have on the phonon density of states (DOS), we compare these in Fig. 1 for the $P2_1$ phase at a pressure of $P = 2$ TPa ($V_0/V = 8.2$); in the same structure, assuming a difference in mass of the hydrogen isotope, changes to the phonon DOS are significant. As one might expect, the high-frequency limit is especially susceptible to the mass changes; the highest phonon bands,

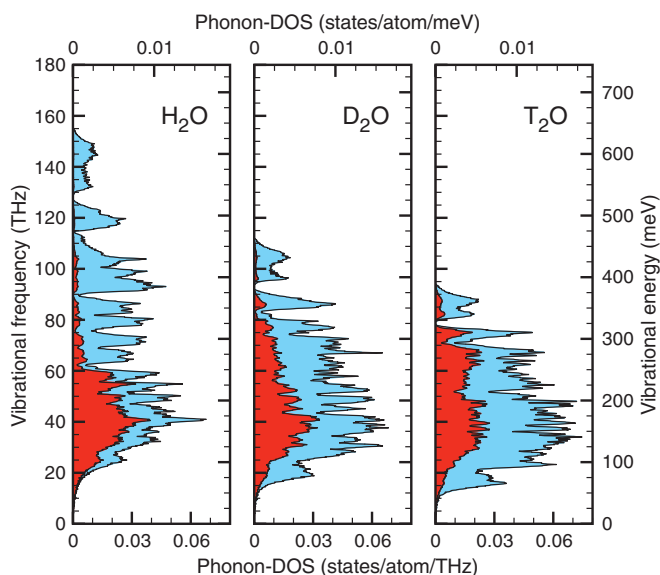


FIG. 1. (Color online) Phonon density of states per atom of $P2_1$ phase of ice at $P = 2$ TPa for various hydrogen isotopes. Colored areas under the curve correspond to the partial O (red/dark grey) and H/D/T (blue/light grey) phonon DOSs (the blue region augmenting the red to give the total). A vibrational frequency of 100 THz corresponds to a vibrational energy of 3335.6 cm^{-1} , or 413.6 meV .

dominated by hydrogen, shift from around 140 THz for H (ca. 4670 cm^{-1} , 580 meV) via 100 THz for D (ca. 3330 cm^{-1} , 413 meV) to about 85 THz for T (ca. 2830 cm^{-1} , 351 meV), these being in very good agreement with a $M^{-1/2}$ scaling behavior. The total ZPEs will be reduced accordingly in heavy water crystals. In fact, these are calculated (in the $P2_1$ phase of ice at $P = 2$ TPa) to be 1.28 eV , 0.99 eV , and 0.86 eV per molecule, respectively.

What do these values signify? The calculated ZPE of an isolated H_2O molecule is 0.56 eV (and $0.41 \text{ eV}/0.32 \text{ eV}$ for $\text{D}_2\text{O}/\text{T}_2\text{O}$, respectively) and, as such, is less than half of the high-pressure values. The ZPE in ice at $P = 1 \text{ atm}$, in the hexagonal ice *Ih* phase, is slightly higher than in the gas phase, 0.69 eV/molecule . With increasing pressure, the ZPE then increases across the molecular phases (for instance, to 0.73 eV/molecule in ice *VIII* at $P = 50 \text{ GPa}$) but decreases again as the transition to atomic ice *X* is approached. This coincides with a lengthening of the intramolecular O-H separations as protons move toward the midpoint of nearest-neighbor O-O connections and the corresponding softening of phonon modes. At $P = 100 \text{ GPa}$ in ice *X*, the ZPE of H_2O -ice is 0.66 eV/molecule , with the shortest O-H distance $d_{\text{OH}} = 1.15 \text{ \AA}$, which is much longer than in the isolated molecule or in ice *VIII*, where $d_{\text{OH}} = 1.03 \text{ \AA}$ at $P = 50 \text{ GPa}$. It requires much higher pressures (700 GPa in the ice *X* phase) to bring all O and H in the solid to within their molecular gas phase separation of $d_{\text{OH}} = 0.97 \text{ \AA}$.

However, only differences in the ZPEs between various ice phases will eventually impact stable phase boundaries, and it is not *a priori* clear how this happens. We now address these differences.

II. STABLE PHASE BOUNDARIES AND THE ISOTOPE EFFECT

We find the following phase transitions for high pressures ices: at $P = 870 \text{ GPa}$, the previously predicted *Pbcm* phase³¹ becomes unstable with respect to a new *Pmc2₁* structure, which at $P = 1170 \text{ GPa}$ then gives way to a $P2_1$ structure as the most stable phase (see Fig. 2 for plots of the relative enthalpies in this pressure region).

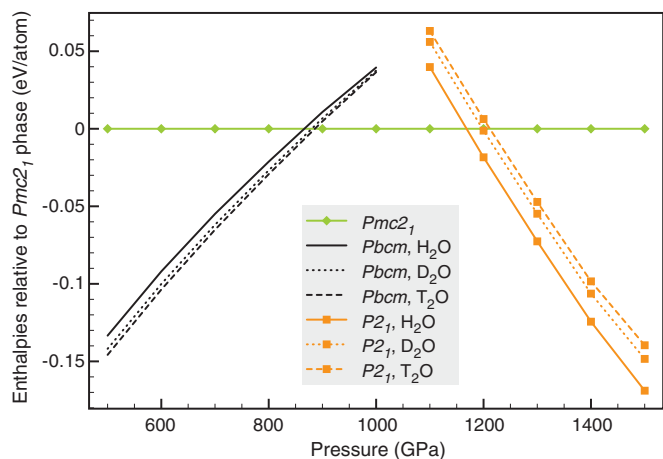


FIG. 2. (Color online) Relative ground-state enthalpies per atom including zero point effects of relevant phases around $P = 1$ TPa, for different hydrogen isotopes.

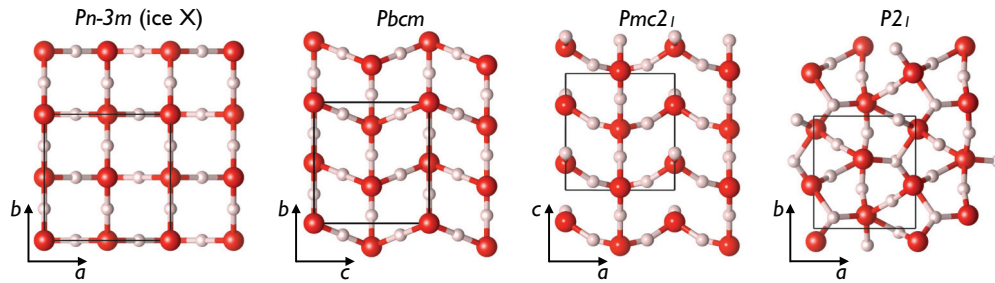


FIG. 3. (Color online) Crystal structures of high-pressure ice phases (all drawn to the same scale). From left: $Pn-3m$ (ice X) at $P = 200$ GPa; $Pbcm$ at $P = 700$ GPa; $Pmc2_1$ at 1.0 TPa; and $P2_1$ at $P = 1.5$ TPa.

The geometries of these structures are fascinating and have been discussed in detail by us elsewhere.⁶ We give an overview of the geometry changes in Fig. 3; all phases are nonmolecular and move beyond the ice X structure through shearing of atomic planes as well as by forming buckled symmetric O-H-O bonds and by increasing the H-coordination of O beyond four and the O-coordination of H beyond two. In combination, all of these effects will lead to more dense structures.

These phases are all wide-gap insulators, with typical static lattice band gaps (computed within DFT) decreasing from 6 eV at $P = 1$ TPa to 2 eV at $P = 4$ TPa. Note that recent work⁵ has suggested a different, more complicated structure of $I-4_2d$ symmetry as a more stable intermediate phase between the $Pbcm$ and the $P2_1$ structures. Other recent work has predicted yet other more stable structures in the terapascal pressure regime^{32,33}; however, we believe the structural features of these high-pressure phases to be sufficiently similar to allow us to draw conclusions from a detailed study of the phases discussed in this paper. These recent calculations also suggest that at pressures beyond those studied here (roughly at $P > 5$ TPa), more hydrogen-rich stoichiometries (i.e., mixtures of ice and hydrogen) could be stabilized.

As previously mentioned, the ZPEs at terapascal pressures are remarkably high across all phases: for H_2O at $P = 1.0$ TPa the ZPE in the $Pbcm$, $Pmc2_1$, and $P2_1$ phases is 1.10 eV, 1.11 eV, and 1.06 eV per formula unit, respectively, at the harmonic level. The ZPEs are thus much higher than the enthalpy differences between the phases. However, since they are all quite similar, the inclusion of the ZPEs still result in only minor changes of the predicted transition pressures (if the system remains crystalline), which would be $P = 930$ GPa for the $Pbcm \rightarrow Pmc2_1$ and $P = 1300$ GPa for the $Pmc2_1 \rightarrow P2_1$ transitions without including the ZPEs.

Since complete omission of ZPEs correspond to an assumption of infinitely massive nuclei, substitution of H by D or T

TABLE I. Zero point energies per molecule and ground-state transition pressures for different isotopes of ice phases relevant around $P = 1$ TPa.

	ZPE at $P = 1$ TPa [eV/molecule]			Upper limit of stability [GPa]			
	H_2O	D_2O	T_2O	H_2O	D_2O	T_2O	No ZPE
$Pbcm$	1.10	0.85	0.74	870	890	895	930
$Pmc2_1$	1.11	0.85	0.73	1170	1200	1210	1300
$P2_1$	1.06	0.81	0.71				

is expected to have an even smaller effect on the transition pressures in this pressure region: both transition pressures increase slightly for the heavier isotopes by about 25 GPa for the $Pbcm \rightarrow Pmc2_1$ transition and about 40 GPa for the $Pmc2_1 \rightarrow P2_1$ transition. The corresponding absolute values are compiled in Table I.

III. HEAVY WATER CRYSTALS NEAR METALLIZATION

Isotope effects have more evident consequences as H_2O , D_2O , and T_2O approach metallization, a fascinating region of the phase diagram but to date inaccessible in terrestrial laboratory settings.

Over a large pressure range the $P2_1$ phase is the most stable, but eventually the $P-1$ and the metallic $C2/m$ phases become more stable (see Figs. 4 and 5 for their structures and relative enthalpies). While the $P-1$ phase is similar to the $P2_1$ phase, with increased coordination both at the O and the H atoms, the $C2/m$ phase is more symmetrical, reciting layered features found, for example, in the lower pressure $Cmcm$ phase.² The region of stability of the $P-1$ phase depends crucially on the choice of isotope: whereas in H_2O , the $P-1$ phase is stable from $P = 3.75$ TPa to $P = 7$ TPa, in T_2O it would be stable only between $P = 4.4$ TPa and $P = 5.0$ TPa. Note that the $P-1$ phase has no region of stability if ZPEs are actually neglected and only static ground-state enthalpies are compared.⁶ The isotope dependence thus in turn affects the onset of metallization of ice because the $C2/m$ phase, which succeeds the $P-1$ phase, is the first metallic ice phase that becomes stable: the heavier the water molecule, the earlier this metallic phase is stabilized, for H_2O only at $P = 7$ TPa but for T_2O already at $P = 5$ TPa. Another consequence of such large isotopic effects is that in certain pressure regions

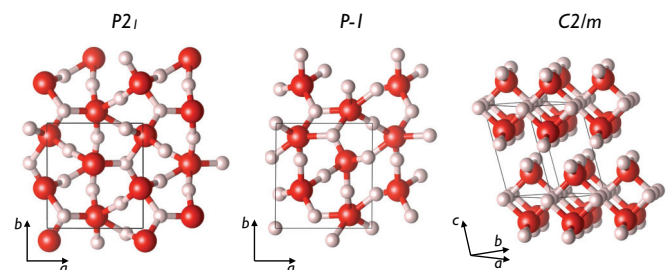


FIG. 4. (Color online) Static ice phases at $P = 5.0$ TPa. From left: $P2_1$ phase, $P-1$ phase, and $C2/m$ phase.

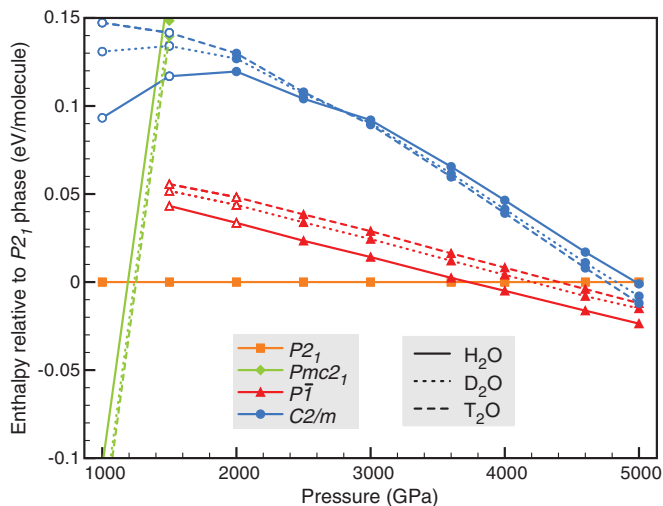


FIG. 5. (Color online) Relative ground-state enthalpies of relevant phases around $P = 5$ TPa given per molecule, including zero point effects, and for different hydrogen isotopes. Open symbols denote the onsets of dynamical instability at low pressures.

different isotopomers may well have different ground states. In the case of ice, at $P = 4$ TPa (a relative compression of about $V_0/V = 11$), H_2O would seem to be stable in the $P-1$ phase, while D_2O would be stable in the $P2_1$ phase.

The quite substantial change in the stability of these phases is only made possible because the trends in ZPEs have opposite signs for different phases. Of the phases shown in Fig. 5, $P-1$ is destabilized with respect to the $P2_1$ phase for heavier hydrogen isotopes, while the others are ultimately stabilized with respect to $P2_1$. Additionally, the enthalpy differences between the most competitive phases are much smaller around $P = 5$ TPa than around $P = 1$ TPa (note the different energy scales in Figs. 2 and 5), while the differences in ZPEs are about the same (see Table II). It is thus also entirely conceivable that an amorphous or even liquid state could be adopted as the ground state of water ice under these conditions; the energy reservoir presented by the ZPE alone could lead to the presence of metastable phases in a macroscopic ice sample. The distinction between the amorphous and liquid state might then be a matter of the existence of collective diffusivity.

IV. STATIC BARRIERS FOR HYDROGEN DIFFUSION

The ZPEs quoted in the previous section are large and may actually provide sufficient energy to facilitate cooperative hy-

TABLE II. Zero point energies per molecule and ground-state transition pressures for different isotopes of ice phases relevant around $P = 5$ TPa (typical compression $V_0/V = 12$).

	ZPE at $P = 5$ TPa [eV/molecule]			Upper limit of stability [TPa]			
	H_2O	D_2O	T_2O	H_2O	D_2O	T_2O	No ZPE
$P2_1$	1.70	1.32	1.15	3.7	4.2	4.4	4.65
$P-1$	1.67	1.30	1.13	~ 7	~ 5.5	5.0	N/A
$C2/m$	1.72	1.33	1.16				

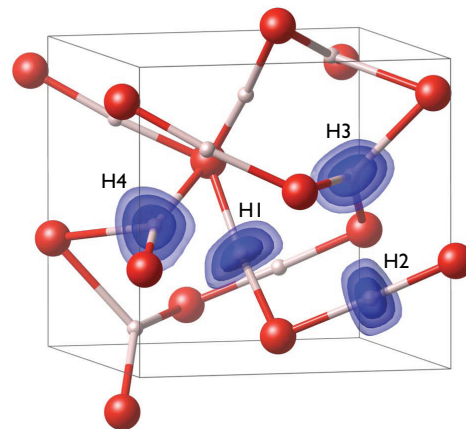


FIG. 6. (Color online) The ground-state static high-pressure $P2_1$ phase at $P = 2$ TPa (compression $V_0/V = 8.2$), shown with three potential energy isosurfaces ($V = 0.5$ eV, 1.0 eV, and 1.5 eV) around the four labeled unique hydrogen lattice sites in the unit cell.

drogen tunneling even at very low temperatures, thus quantum melting of the hydrogen sublattice. The static structures we calculated as possessing the lowest enthalpy for H_2O at very high pressures contain O-H-O-H-O- motifs that are suggestive of potential correlated motions in the lattice—these are the focus of the next phase of our study.

In particular we wanted to establish first how much enthalpy might be involved in the displacements of single independent hydrogens. As an example, we show in Fig. 6 the potential energy surfaces experienced by the protons in the $P2_1$ phase at $P = 2$ TPa. For each of the four unique H lattice sites in the unit cell, we systematically displaced the protons on a regular grid away from their lattice sites (keeping all other ions fixed in their previously optimized positions) in order to map out the potential energy surface for each site. Figure 6 thus compiles the results from four independent sets of calculations, one for each hydrogen atom lattice site. Several iso-surfaces (of roughly ellipsoidal character) of the potential energy are shown, the outermost representing a barrier of 1.5 eV above the potential energy minimum occurring at the actual hydrogen lattice sites.

Not surprisingly, the potential energy rises fastest along the quasilinear O-H-O bonds (the three iso-surfaces are close to each other) and is slowest in the planes perpendicular to these bonds. Threefold coordinated protons experience markedly shallower potentials than twofold coordinated protons.

If, in the harmonic approximation, we calculate the isolated vibrations of the individual protons in each of these potentials (using a $2 \times 2 \times 2$ supercell to avoid spurious interactions between image sites), we obtain frequencies ranging from 1870 cm^{-1} to 4100 cm^{-1} and corresponding ZPEs between 467 meV and 550 meV for the different sites. These ZPE values compare well to the 0.49 eV obtained from projecting the actual phonon DOS onto the hydrogen atoms, as carried out in Fig. 1. In the harmonic approximation, the frequencies and energies of deuterium or tritium are easily obtained by scaling with the inverse root of the mass ratio. In the ground state, the average ZPE of about 0.52 eV per proton would not be sufficient for a proton to leave the local minimum of any

TABLE III. Parameters and results of harmonic fits of the potential energy surfaces around individual hydrogen sites in the $P2_1$ phase at $P = 2$ TPa. Root mean square displacement (RMSD) $\langle u^2 \rangle^{1/2}$ of individual protons in the vibrational ground state and root mean square error (RMSE) of the harmonic fit to the potential energy surface are given.

Hydrogen site	ZPE (eV/atom)		Ionic wave function RMSD $\langle u^2 \rangle^{1/2}$ (Å)	Harmonic fit indicators	
	Harmonic PES fit	DFT phonon calculations		R^2	RMSE (eV)
H1	0.490	0.550	0.144	0.990	0.068
H2	0.501	0.529	0.139	0.995	0.046
H3	0.421	0.524	0.152	0.978	0.099
H4	0.428	0.467	0.150	0.984	0.083

of the hydrogen lattice sites. In fact, the spatial uncertainty of each proton caused by the zero point excursion is given (in the harmonic approximation) by the iso-surface of the potential energy corresponding to its ZPE and is thus about the size of the innermost iso-surface shown in Fig. 6, which is drawn at a potential height of 0.5 eV.

To assess whether the harmonic approximation is at all applicable under these conditions of high compression, we fit the potential energy surface for each hydrogen lattice site to an anisotropic harmonic oscillator. Quality parameters of each fit, together with the respective energy of the harmonic ground state and the dimension of its wave function, are listed in Table III.

It will be noted that the potential energy surface is reasonably well described through the harmonic ansatz and that the potential energy surfaces of hydrogens in quasilinear O-H-O arrangements (H1 and H2) follow the harmonic model significantly better than the quasitriply coordinated hydrogens (H3 and H4). The latter experiences larger root mean square (RMS) displacements. But it is clear that at larger displacements anharmonic terms must come into play. This can be seen in Fig. 7, where we plot the potential energy for two different hydrogen sites (H1 and H4) along the principal axes of their respective harmonic oscillator fits. In both cases, a fourth-order fit of the energy as a function of the atomic displacements is more appropriate than a harmonic approach.

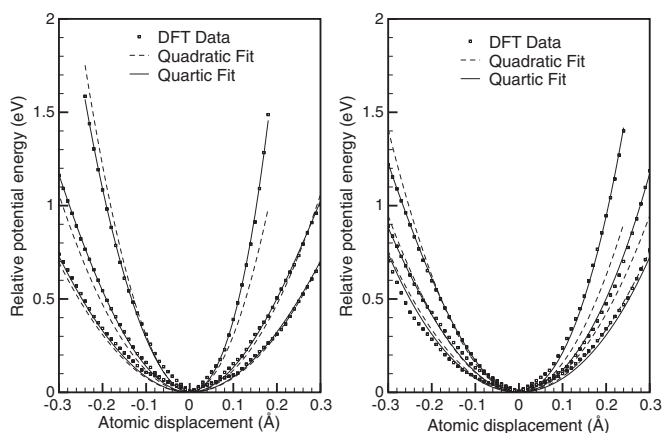


FIG. 7. Potential energy curves for displacements of individual hydrogen atoms in the $P2_1$ phase at $P = 2$ TPa along the principal axes of the best harmonic oscillator fit of the three-dimensional potential energy surface. Left: hydrogen site H1; right: hydrogen site H4 (see Fig. 6).

Note that the displacement axis ranges in Fig. 7 correspond to about twice the actual RMS displacements of protons in the ground state, which are around 0.15 Å.

Do these large excursions imply the possibility of quantum melting of the hydrogen sublattice? The classical Lindemann criterion suggests melting of a material, if the (thermal) RMS displacement reaches 10–15% of the interatomic distance.^{34–36} In quantum systems, such as solid ^4He , the corresponding threshold seems to be closer to 25–30% of the interatomic distance.^{37–39} Typical proton RMS displacements at $P = 2$ TPa of ~ 0.15 Å (compared to typical nearest-neighbor H-H separations, $d_{\text{NN}} = 1.0$ – 1.2 Å) therefore reach the classical Lindemann melting threshold but fall short of the accepted threshold for quantum systems. Quantum melting of the hydrogenic sublattice thus seems unlikely. In heavy waters, with smaller RMS displacements of 0.13 Å (D_2O) and 0.11 Å (T_2O), this seems to be reinforced.

Interestingly, higher pressure does not necessarily lead to a larger tendency toward sublattice melting. In Fig. 8, we show the ratio of the RMS displacements $\langle u^2 \rangle^{1/2}$ to the nearest-neighbor separation d_{NN} for different ice phases and as a function of pressure. These were obtained from quasiharmonic phonon calculations. Over the entire pressure range studied, from $P = 1$ – 5 TPa, the proton displacement is about $16 \pm 2\%$ of the nearest-neighbor separation, with little variation. Higher

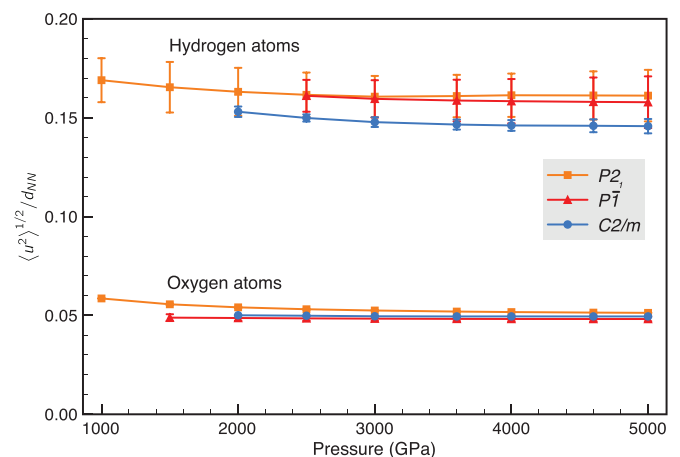


FIG. 8. (Color online) Zero-point RMS atomic displacements in different high-pressure ice phases, relative to nearest-neighbor separations d_{NN} . Error bars denote a range of such values associated with different atomic sites in the unit cell. Both O and H displacements are shown.

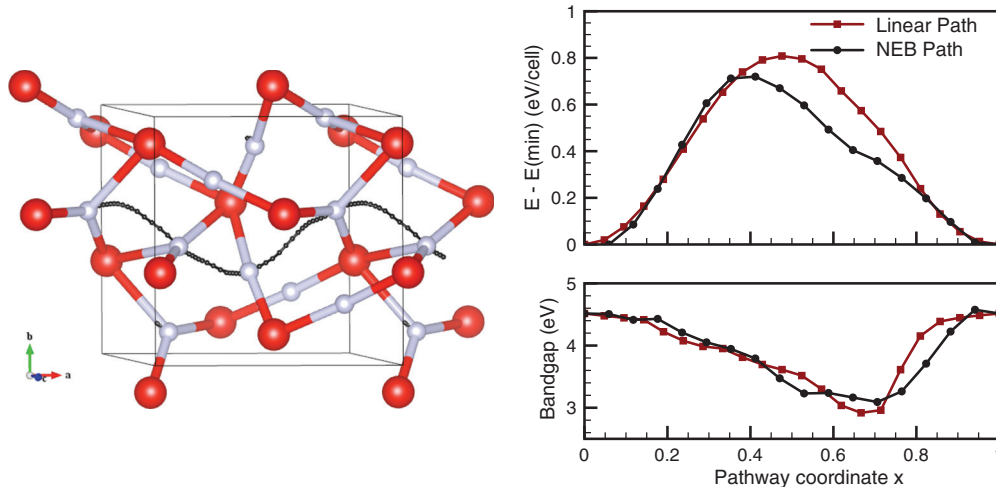


FIG. 9. (Color online) Coherent proton diffusion through the $P2_1$ phase at $P = 2$ TPa. Left: schematic of coherent diffusion; black beaded line indicates the optimized nudged elastic band (NEB) path. Right: energy profile along the diffusion path and the electronic band gap along the path.

pressures lead to more compact structures, but steeper ionic potential energy surfaces also lead to more compact vibrational wave functions and, in the process, to much increased ZPEs.

V. CONCERTED HYDROGEN MOTIONS: A POSSIBILITY

As we just saw, the ZPE reservoir at high pressure is immense but so are the barriers preventing melting of the hydrogenic sublattice. However, diffusive motion of protons through the lattice might nevertheless be expected to occur in a coherent or concerted way and not through an independent hopping motion; the easiest targets for proton diffusion would then be neighboring hydrogen lattice sites, which in turn would need to be cooperatively vacated by their initial inhabitants. This is different from low-pressure molecular ice phases and around the boundary to atomic ice X , where ice structures are open enough to feature empty lattice sites that individual protons could migrate into as part of a diffusional process.^{40,41} In fact, partial occupancy of octahedral sites in ice VII (away from nearest-neighbor O-H-O connections) has been proposed to explain recent high-pressure neutron studies of ice around $P = 50$ GPa.²⁰ And both neutron diffraction experiments⁴² and path integral molecular dynamics calculations⁴³ have hinted at possible concerted hydrogen diffusion in molecular ice phases.

To simulate coherent or concerted diffusion, we forced one of the protons in the $P2_1$ unit cell along a linear path toward its neighboring hydrogen lattice sites, in the process allowing all other protons to freely relax but keeping the O sublattice fixed. This nudged diffusion then results in various energy profiles $E(x)$ (where $x = 0$ and $x = 1$ correspond to the initial and final states), which should be reasonably close to the optimal path along the potential energy surface. We chose the path with the lowest activation barrier and reoptimized it using the Nudged Elastic Band (NEB)⁴⁴ method, thereby approaching the actual transition path closest to our initial choice of a linear pathway.

The energetically most favorable pathway is now shown in Fig. 9, together with a diagram indicating the coherent proton motion: in this particular process, protons are now diffusing

along a chain in the a direction through the crystal, with three out of eight protons in the unit cell involved in the diffusion process, while the others remain in place. Along the whole path, if one assumes an adiabatic response of the electronic states to the ionic motion, the structure will remain insulating, albeit with a band gap that is reduced by up to 1.5 eV (see Fig. 9).

In contrast to proton tunneling in the low-pressure molecular phases, which is expected to occur along O-H-O bonds, in near classical terms a proton diffusing in these close-packed high-pressure phases must leave the O-H-O bond and then move into another hydrogen lattice site. The barrier for this coherent motion is about 0.7 eV per unit cell, or 0.175 eV per water molecule; this is much smaller than the ZPE available at a pressure of $P = 2$ TPa, which as we remember is in the harmonic approximation about 1.28 eV (0.99 eV, 0.86 eV) per H_2O (D_2O , T_2O) molecule. It is therefore again not unreasonable to assume that under the extreme conditions of terapascal pressures (or relative compressions of around $V_0/V \sim 10$), the hydrogenic sublattice of ice could indeed melt, i.e., take on a diffusive state, with the oxygen sublattice remaining crystalline. This effect will clearly depend on the mass of the hydrogen isotope, and this could possibly be detected through shock wave experiments. There might well be a pressure range where hydrogen in compressed H_2O is diffusive, whereas deuterium in compressed D_2O is not. In future work, we intend to model this dynamic (the quantum nature of the hydrogens could be better accounted for by performing path integral molecular dynamics calculations⁴⁵) but also to proceed beyond the harmonic approximation. One possible avenue involves the development of suitable effective pair interaction potentials to describe the ionic potential energy surface of the high-pressure phases²⁷ and their application within one of the implementations of the self-consistent harmonic approximation.⁴⁶⁻⁴⁹

VI. SUMMARY

We have investigated in detail the dynamical properties of recently proposed new high-pressure ice phases, especially

to extract isotopic effects on stable phase boundaries and also the possible melting of the hydrogen sublattice, even at low temperatures. Within the harmonic approximation, we find that regions of stability for various phases around $P = 5$ TPa (near metallization) are greatly influenced by the choice of hydrogen isotope. The onset of metallization in pressurized ice could thus be quite different for the heavy waters.

Turning to a microscopic picture for proton migration and sublattice melting, we have also found in our computations that the barriers for concerted hydrogen diffusion in H_2O in the terapascal pressure regime are rather low. It is possible that the ground state of ice in these conditions is a superionic phase. While our conclusions are somewhat speculative, they nevertheless point in several ways to classical or quantum mobility of hydrogen containing sublattices in H_2O under

pressure. Even at extremely high pressures, with few nooks and crannies left, H_2O may be a fluid, though a very different kind than its life-enhancing form in one atmosphere.

ACKNOWLEDGMENTS

Support for our work comes from EFree, an Energy Frontier Research Center funded by the U.S. Department of Energy (Award No. DESC0001057 at Cornell) and the National Science Foundation through Grants No. DMR-0907425 and No. CHE-0910623. Computational resources provided by the Cornell NanoScale Facility (supported by the National Science Foundation through Grant No. ECS-0335765) and by the XSEDE network (provided by the National Center for Supercomputer Applications through Grant No. TG-DMR060055N) are gratefully acknowledged.

*Corresponding author: a.hermann@ed.ac.uk

¹V. F. Petrenko and R. W. Whitworth, *Physics of Ice* (Oxford University Press, Oxford, 1999).

²B. Militzer and H. F. Wilson, *Phys. Rev. Lett.* **105**, 195701 (2010).

³J. M. McMahon, *Phys. Rev. B* **84**, 220104 (2011).

⁴M. Ji, K. Umemoto, C. Z. Wang, K. M. Ho, and R. M. Wentzcovitch, *Phys. Rev. B* **84**, 220105 (2011).

⁵Y. Wang, H. Liu, J. Lv, L. Zhu, H. Wang, and Y. Ma, *Nature Commun.* **2**, 563 (2011).

⁶A. Hermann, N. W. Ashcroft, and R. Hoffmann, *Proc. Natl. Acad. Sci.* **109**, 745 (2012).

⁷R. Hoffmann, *Am. Sci.* **100**, 260 (2013).

⁸C. Cavazzoni, G. L. Chiarotti, S. Scandolo, E. Tosatti, M. Bernasconi, and M. Parrinello, *Science* **283**, 44 (1999).

⁹N. Goldman, L. E. Fried, I.-Feng W. Kuo, and C. J. Mundy, *Phys. Rev. Lett.* **94**, 217801 (2005).

¹⁰M. French, T. R. Mattsson, N. Nettelmann, and R. Redmer, *Phys. Rev. B* **79**, 054107 (2009).

¹¹A. F. Goncharov, N. Goldman, L. E. Fried, J. C. Crowhurst, I.-Feng W. Kuo, C. J. Mundy, and J. M. Zaug, *Phys. Rev. Lett.* **94**, 125508 (2005).

¹²E. Schwegler, M. Sharma, F. Gygi, and G. Galli, *Proc. Natl. Acad. Sci.* **105**, 14779 (2008).

¹³R. B. Firestone and S. Y. Frank Chu, *Table of Isotopes*, 8th ed. (Wiley-Interscience, New York, 1998).

¹⁴J. E. Schirber, J. M. Mintz, and W. Wall, *Solid State Commun.* **52**, 837 (1984).

¹⁵R. Cornog and W. F. Libby, *Phys. Rev.* **59**, 1046 (1941).

¹⁶W. F. Libby, *Phys. Rev.* **69**, 671 (1946).

¹⁷W. B. Hubbard, W. J. Nellis, A. C. Mitchell, N. C. Holmes, S. S. Limaye, and P. C. McCandless, *Science* **253**, 648 (1991).

¹⁸R. M. C. Lopes, K. L. Mitchell, E. R. Stofan, J. I. Lunine, R. Lorenz, F. Paganelli, R. L. Kirk, C. A. Wood, S. D. Wall, L. E. Robshaw, A. D. Fortes, C. D. Neish, J. Radebaugh, E. Reffet, S. J. Ostro, C. Elachi, M. D. Allison, Y. Anderson, R. Boehmer, G. Boubin, P. Callahan, P. Encrenaz, E. Flamini, G. Francescetti, Y. Gim, G. Hamilton, S. Hensley, M. A. Janssen, W. T. K. Johnson, K. Kelleher, D. O. Muhleman, G. Ori, R. Orosei, G. Picardi, F. Posa, L. E. Roth, R. Seu, S. Shaffer, L. A. Soderblom, B. Stiles, S. Vetrilla, R. D. West, L. Wye, and H. A. Zebker, *Icarus* **186**, 395 (2007).

¹⁹L. Dubrovinsky, N. Dubrovinskaia, V. B. Prakapenka, and A. M. Abakumov, *Nat. Commun.* **3**, 1163 (2012).

²⁰M. Guthrie, R. Boehler, C. A. Tulk, J. J. Molaison, A. M. dos Santos, K. Li, and R. J. Hemley, *Proc. Natl. Acad. Sci.* **110**, 10552 (2013).

²¹J. H. Eggert, D. G. Hicks, P. M. Celliers, D. K. Bradley, R. S. McWilliams, R. Jeanloz, J. E. Miller, T. R. Boehly, and G. W. Collins, *Nat. Phys.* **6**, 40 (2009).

²²D. K. Bradley, J. H. Eggert, R. F. Smith, S. T. Prsbrey, D. G. Hicks, D. G. Braun, J. Biener, A. V. Hamza, R. E. Rudd, and G. W. Collins, *Phys. Rev. Lett.* **102**, 075503 (2009).

²³B. Weaver, J. Rabovsky, and P. O'Connell, *DOE Handbook Tritium Handling and Safe Storage* (US Department of Energy, Washington, DC, 2008).

²⁴D. J. Hooton, *Philos. Mag.* **3**, 49 (1958).

²⁵N. S. Gillis, N. R. Werthamer, and T. R. Koehler, *Phys. Rev.* **165**, 951 (1968).

²⁶D. M. Straus and N. W. Ashcroft, *Phys. Rev. Lett.* **38**, 415 (1977).

²⁷B. Edwards, N. W. Ashcroft, and T. Lenosky, *Europhys. Lett.* **34**, 519 (1996).

²⁸D. Alfè, *Comput. Phys. Commun.* **180**, 2622 (2009).

²⁹G. Kresse and J. Furthmüller, *Phys. Rev. B* **54**, 11169 (1996).

³⁰A. Togo, F. Oba, and I. Tanaka, *Phys. Rev. B* **78**, 134106 (2008).

³¹M. Benoit, M. Bernasconi, P. Focher, and M. Parrinello, *Phys. Rev. Lett.* **76**, 2934 (1996).

³²C. J. Pickard, M. Martinez-Canales, and R. J. Needs, *Phys. Rev. Lett.* **110**, 245701 (2013).

³³S. Zhang, H. F. Wilson, K. P. Driver, and B. Militzer, *Phys. Rev. B* **87**, 024112 (2013).

³⁴F. A. Lindemann, *Phys. Z.* **11**, 609 (1910).

³⁵T. V. Ramakrishnan and M. Yussouff, *Phys. Rev. B* **19**, 2775 (1979).

³⁶S. Rabinovich, D. Berrebi, and A. Voronel, *J. Phys.: Condens Matter.* **1**, 6881 (1989).

³⁷P. A. Whitlock, D. M. Ceperley, G. V. Chester, and M. H. Kalos, *Phys. Rev. B* **19**, 5598 (1979).

³⁸S. T. Chui, *Phys. Rev. B* **41**, 796 (1990).

³⁹C. A. Burns and E. D. Isaacs, *Phys. Rev. B* **55**, 5767 (1997).

- ⁴⁰M. Benoit, D. Marx, and M. Parrinello, *Nature* **392**, 258 (1998).
- ⁴¹E. Katoh, H. Yamawaki, H. Fujihisa, M. Sakashita, and K. Aoki, *Science* **295**, 1264 (2002).
- ⁴²L. E. Bove, S. Klotz, A. Paciaroni, and F. Sacchetti, *Phys. Rev. Lett.* **103**, 165901 (2009).
- ⁴³L. Lin, J. A. Morrone, and R. Car, *J. Stat. Phys.* **145**, 365 (2011).
- ⁴⁴G. Mills, H. Jónsson, and G. K. Schenter, *Surf. Sci.* **324**, 305 (1995).
- ⁴⁵D. Marx and M. Parrinello, *J. Chem. Phys.* **104**, 4077 (1996).
- ⁴⁶D. J. Hooton, *Z. Phys.* **142**, 42 (1955).
- ⁴⁷T. Koehler, *Phys. Rev. Lett.* **17**, 89 (1966).
- ⁴⁸D. Stroud and N. W. Ashcroft, *Phys. Rev. B* **5**, 371 (1972).
- ⁴⁹J. F. Dobson, *Phys. Lett. A* **62**, 368 (1977).